

RSC Advances



This is an *Accepted Manuscript*, which has been through the Royal Society of Chemistry peer review process and has been accepted for publication.

Accepted Manuscripts are published online shortly after acceptance, before technical editing, formatting and proof reading. Using this free service, authors can make their results available to the community, in citable form, before we publish the edited article. This *Accepted Manuscript* will be replaced by the edited, formatted and paginated article as soon as this is available.

You can find more information about *Accepted Manuscripts* in the [Information for Authors](#).

Please note that technical editing may introduce minor changes to the text and/or graphics, which may alter content. The journal's standard [Terms & Conditions](#) and the [Ethical guidelines](#) still apply. In no event shall the Royal Society of Chemistry be held responsible for any errors or omissions in this *Accepted Manuscript* or any consequences arising from the use of any information it contains.

Dynamic Mechanical Properties of Multiwall Carbon Nanotube Reinforced ABS Composites and its Correlation with Entanglement Density, Adhesion, Reinforcement and C Factor

Jeevan Jyoti^{1,2}, Bhanu Pratap Singh^{1,2*}, Abhishek K. Arya¹, S.R Dhakate¹

¹Physics and Engineering of Carbon, Division of Materials Physics and Engineering

²Academy of Scientific and Innovative Research (AcSIR),

CSIR-National Physical Laboratory, New Delhi-11012, India

Abstract

The dynamic mechanical properties of multiwalled carbon nanotube (MWCNTs) reinforced acrylonitrile butadiene styrene (ABS) high performance composites prepared by micro twin screw extruder with back flow channel which enable proper dispersion of MWCNTs into polymer matrix are studied in detail. The dynamic characteristics of MWCNTs/ABS composites such as storage, loss modulus and damping factor were significantly affected with the incorporation of MWCNTs. The dynamic mechanical properties of polymers strongly depend on the adhesion of MWCNTs and polymer and entanglement density of polymer chains in presence of MWCNTs. Herein, entanglement density and C-factor have been evaluated by using dynamic mechanical properties results obtained from dynamic mechanical analyser and correlated with their mechanical properties. Entanglement density of the MWCNT/ABS composites is increased from 4.31×10^{-4} mol/m³ (pure ABS) to 7.6×10^{-4} mol/m³ (5wt.% MWCNT/ABS composites). C-factor measures the effectiveness of the filler on the modulus of the composites which decreased from 1.086 (1 wt.% MWCNT/ABS composites) to 0.78 (5 wt.% MWCNT/ABS composites) and beyond this loading the value of C-factor start increasing which showed that the utilization of 5wt% MWCNTs in ABS matrix is sufficient for their effective use. The “b” factor increased from 6.16 (1 wt. % MWCNTs/ABS composites) to 7.625 (5 wt.% MWCNT/ABS composites) after that start decreasing. Greater the value of “b” leads to strengthen the MWCNTs/ABS matrix interaction. Additionally, Cole- Cole analysis has been carried out to understand the phase behaviour of the composites.

Keywords: Multiwall Carbon Nanotube (MWCNTs), Acrylonitrile Butadiene Styrene (ABS), Storage modulus (E'), loss modulus (E''), glass transition temperature (T_g),

Corresponding author: Tel.: +91-11-45608460; Fax: +91-11-45609310

Email Address: [*bps@nplindia.org](mailto:bps@nplindia.org), bpsingh2k4@yahoo.com (B.P. Singh)

Introduction

Polymers reinforced with carbon nanotubes have received a great attention towards the research community in recent years due to superior mechanical properties of the carbon nanotubes (CNTs)^{1, 2}. Dynamic mechanical analyzer (DMA) commonly referred to evaluate the stiffness and damping properties of a composite's material. The study of structural and the viscoelastic behaviours of the polymeric materials are used for industrial applications of these materials. DMA also determines the primary relaxation of the composites material like a glass transition temperature (T_g), degree of the entanglement, adhesion factor and non Arrhenius variation of the relation with the temperature³⁻⁶. Various aspects of the structural properties like T_g of polymer influence different properties like fatigue and impact resistance. The T_g serves as a transition point between glassy and rubbery region. Glassy region (below T_g) is mainly used to study the structural property of the composite materials.

Properties of the composites materials highly depend upon the type of the filler, its dimensions and aspect ratio as well as filler incorporation technique. There are mainly three types of incorporation techniques: melt mixing⁷⁻⁹, solvent casting¹⁰⁻¹⁴ and in-situ polymerization¹⁵⁻¹⁸. For the industrial viability melt mixing is one of the most preferred techniques for the incorporation of filler in polymer matrix.

In the recent breakthroughs in nanoscale science and engineering has provided new opportunities for the development of high-performance composite materials. Carbon nanotubes (CNTs) have showed the exceptional properties like high mechanical and electrical properties¹⁹⁻²⁵. CNT polymer composites have showed the remarkable increase in the elastic modulus and strength because of the addition of the MWCNTs²⁶⁻³⁰.

Dynamic mechanical analyses are expressed in terms of the storage modulus, loss modulus and the damping factor which depends upon the time (temperature). Addition of the MWCNTs in the polymeric matrix reduces the mobility of the macromolecular chain of polymer surrounding the MWCNTs³¹.

In DMA, a sinusoidal force is applied which measure the response of the input. The behaviour of the material depends upon the response of the output signal. In DMA stress is applied as the function of time (temperature), and the relation with the frequency is given by³²

$$\sigma(t) = \sigma_0 \sin(\omega t + \delta) \quad (1)$$

By using the Hooke's law, the input and response are related by the dynamic modulus

$$\sigma(t) = E^*(\omega)(t) \quad (2)$$

The dynamic modulus has in phase and out of the phase components, and is given by

$$E^*(\omega) = E'(\omega) + iE''(\omega) \quad (3)$$

Where $E' = \left(\frac{\sigma_0}{\epsilon_0}\right)\cos\delta$ is the in real phase and characterizes the elastic behaviour of the composites and the out of the phase $E'' = \left(\frac{\sigma_0}{\epsilon_0}\right)\sin\delta$ characterizes the viscous behaviour of the material³³. Viscoelastic behaviour is the combination of both the viscous and elastic modulus of the material. In DMA, specimen can be tested in different mode of the configuration like single cantilever, dual cantilever, three points bending, torsion, tension, etc.

Several works have been reported on the DMA of synthetic fiber reinforced polymer composites³⁴⁻³⁶. All these authors have mainly focused on the importance of fiber loading (wt. %) in the polymer. Etaati et al.³⁷ studied the static and visco-elastic behaviour of short hemp fiber polypropylene composites manufactured by injection moulding technique. The result showed that increase in storage modulus was negligible in the composites reinforced more than 40 wt% of hemp fibers. Jawaaid et al.³⁸ studied the interfacial bonding between the oil palm–epoxy composites. Addition of jute fibres to oil palm composite increases the storage modulus while damping factor shifts towards higher temperature region. Cole–Cole analysis was made to understand the phase behaviour of the composite samples. The hybrid composite with oil

palm:jute (1:4) showed maximum damping behaviour and highest tensile properties. In another study by Karaduman et al.,³⁹ the magnitudes of peak storage modulus and loss modulus of nonwoven composites improved with an increase in the jute fiber content.

Khare et al.⁴⁰ studied the effect of MWCNTs dispersion in epoxy polymer composites. The result showed that the polymer composites containing the higher dispersion of MWCNTs have greater T_g as compared to the pure epoxy. Babal et al.⁹ studied the effect of MWCNTs and functionalized CNTs (FCNTs) on polycarbonate (PC) polymer composites. They studied the DMA and mechanical properties of MWCNTs and FCNTs. The result showed that the lower value of T_g of CNTs composites as compare to pure PC. Kumar et al.⁴¹ studied the dynamic mechanical properties of MWCNTs/Poly(Acrylonitrile styrene-butadiene)/epoxy hybrid composites. The DMA of the blend composite materials gave two different T_g values: one corresponding to epoxy- and other corresponds an ABS-rich phase, which confirms the two-phase morphology in blends. For hybrid composites, MWCNTs localize in epoxy phase and ABS phase. The improvement in storage modulus by the addition of nanofillers provided better load bearing capacity for the composites. The thermal and dimensional stability of the hybrid composites are comparable with that of neat cross linked epoxy and the blend. Hatui et al.⁴² studied the storage modulus (E') and T_g of the ABS which were significantly increased with the addition of modified MWCNTs as compared to unmodified MWCNTs.

DMA of the polymer and CNTs polymer composites materials has provided the information regarding the T_g and E' in the previous studies. For the processing of the CNT/polymer composites at the industrial scale the entanglement density, adhesion and C factor are very important. The main aim of this work is to investigate the interfacial adhesion, adhesion factor, efficiency factor and reinforcement behaviour of the CNT based ABS polymer composites using DMA. The adhesion behaviour and reinforcement properties are crucial to determine the efficiency of CNTs and the structural stability of the polymer composites.

Materials

In this study, the ABS granules were used as a polymer matrix. By employing catalytic chemical vapour deposition technique, MWCNTs were produced by thermal decomposition of toluene as

carbon source in a long quartz tube heating at constant temperature under the inert atmosphere and ferrocene used as a catalyst. The details about the experimental set-up are given elsewhere⁴³.

Preparation of MWCNTs/ ABS Nanocomposites

ABS polymer granules were dried for a minimum of 10 hours heated at 95°C in the vacuum oven to remove the moisture trapped within the polymer matrix. MWCNTs/ABS nanocomposites containing 0, 1,3,5,7 and 10 wt% of MWCNTs was prepared by HAAKE Mini Lab II Micro compounder. In the compounder, ABS granules were softened and the proper mixing of the MWCNTs with the help of the co-rotating screw in the extrusion with speed of 100 rpm and the mixing time 3 min for each sample was taken place. The mixed material was transferred to a mold and then presses by applying pressure of 670 bars to get the desired shape. Nanocomposites were made from different weight percentage of MWCNTs loading in the ABS polymer matrix (1, 3, 5, 7 and 10 wt %) and designated as ABS-1, ABS-3, ABS-5; ABS-7 and ABS-10. A pure ABS, sample was also prepared under the similar condition and designated as ABS-0. The schematic representation of whole process is given in figure 1.

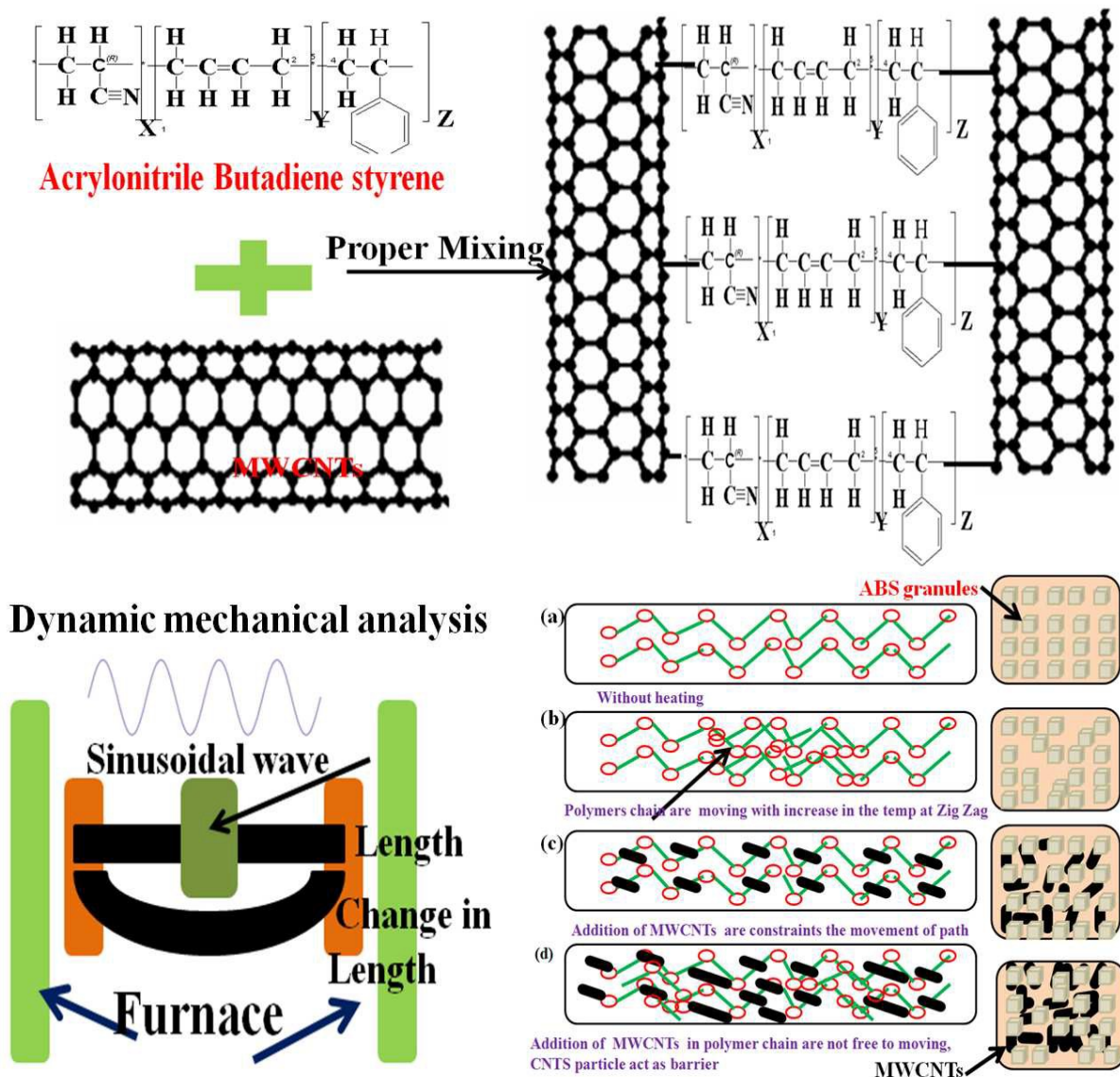


Fig. 1 Schematic representation of mixing of MWCNTs and ABS, interaction of the MWCNTs and ABS and DMTA studies with variation of the temperature.

Characterization

Dynamical mechanical analysis of the ABS and MWCNT/ABS nanocomposites were carried out by the dynamic mechanical thermal analyzer (Perkin Elmer DMA 8000 instruments). Rectangular specimens of $15.75 \times 5.80 \times 3.23 \text{ mm}^3$ [Length \times breadth \times thickness] were used to the analysis. These analyses were done by dual bend cantilever mode in the frequency range of 1 Hz. For the analysis, samples were heated from room temperature to 180°C at heating rate 2°C min^{-1}

Morphology

The Scanning Electron Microscope (SEM) is used for the investigation of the microstructure of MWCNTs/ABS nanocomposites. Fractured surface of the nanocomposites were studied by SEM (model EVO MA10 ZIESS) after tensile fracture of the samples.

Result and discussion

SEM studies are carried out to investigate the surface morphology of the fractured surface and distribution of MWCNTs in ABS. SEM images of ABS-5 and ABS-10 are shown in Figure 2. The SEM images clearly showing the distribution of MWCNTs in the ABS matrix.

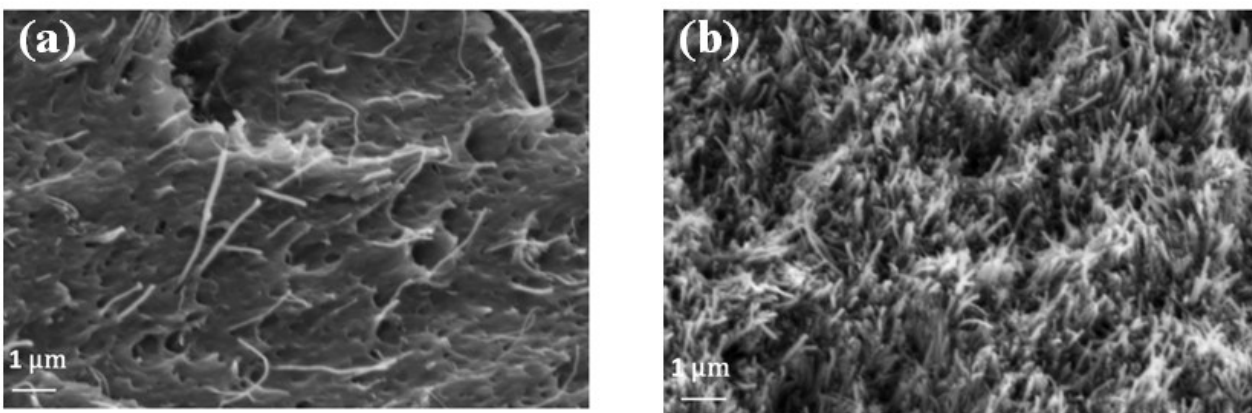


Fig. 2 SEM images of (a) ABS-5 and (b) ABS-10 composites.

Dynamic mechanical analysis

DMA is used to study T_g of polymer and polymer nanocomposites. The storage modulus, (E') signifies the stiffness of the polymer composites. Storage modulus curves show three different regions: high modulus region is glassy region where the segmental mobility is very limited, after that decrease in the value of E' with increase in the temperature also known as transition zone and a rubbery region (the flow region).

Storage modulus

The dynamic storage modulus (E') is proportional to the energy stored per cycle. It is generally equal to the elastic modulus for single, rapid stress at small load and reversible deformation. The

variations in the storage modulus as a function of temperature for the ABS and CNT/ABS composites are shown in Figures 3.

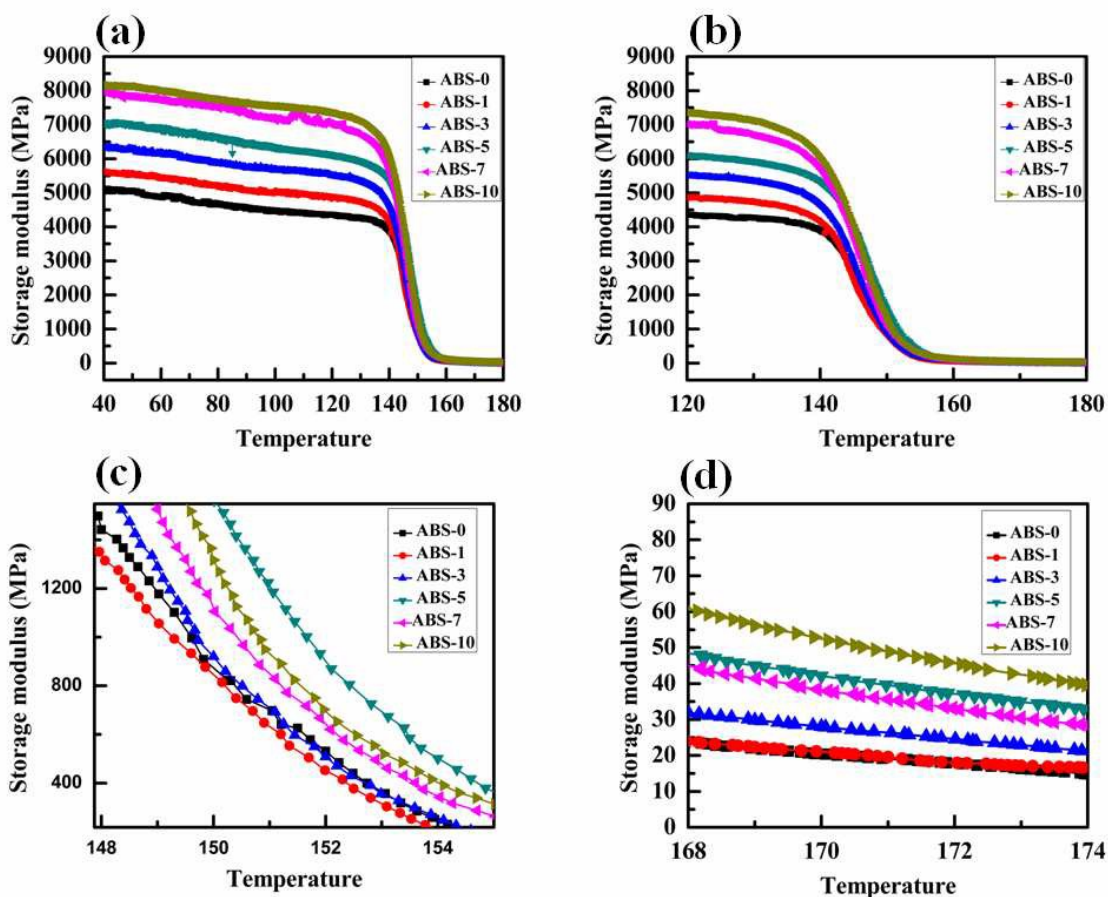


Fig 3 Variation of (a) Storage modulus with temperature, zoomed plot (b) between 120 to 180°C , (c) between 148 to 155°C, (d) between 168 to 174°C for different wt % of MWCNTs/ABS composites

As the temperature increased, the value of E' decreased for all polymer composites, and this was attributed due to the increase in the molecular mobility of the polymer chains⁴⁴. The value of E' of ABS-10 was much higher than ABS-0 at the same temperature. This increase of E' with the addition of MWCNTs was due to the increase in the interfacial adhesion⁴⁵. The drop of the modulus around the glass transition temperature was large for the pure polymer. The difference between the E' values in the glassy and the rubbery state is smaller for composites with higher weight % of MWCNTs. The effect of the MWCNTs on the composites, i.e its effectiveness can be better represented by the coefficient “C” in equation (1)⁴⁶

$$C = \frac{(E'_g/E'_r)_{\text{composites}}}{(E'_g/E'_r)_{\text{pure}}} \quad (4)$$

Where E_g and E_r are the value of storage modulus in the glassy region (130°C) and rubbery region (170°C) respectively. The coefficient “C” parameter is a relative measurement of the decrease in modulus when temperature increases and the material passes through its glass transition. The region of the glassy state is mainly determined the strength of the intermolecular force, and the system of the polymer chain is packed⁴⁶.

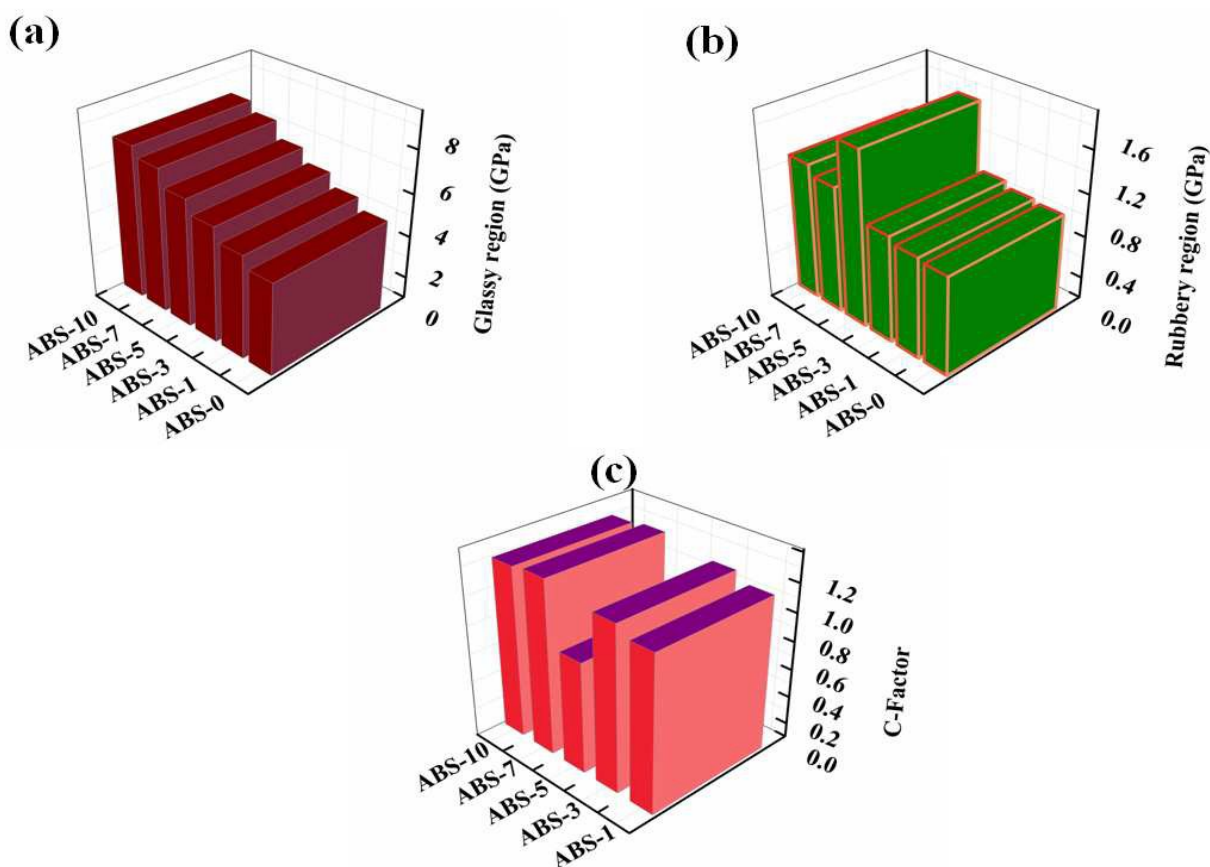


Fig 4. Variation in (a) storage modulus in the glassy region (130°C) (b) storage modulus in the rubbery region (150°C) and (c) Coefficient of “C” factor with the weight percentage of MWCNTs in ABS matrix

A high value of C indicates the less effectiveness of the filler. The value obtained from the different wt% of MWCNTs loading in ABS at frequency 1 Hz is given as Figure 4. The less value of the “C” indicated that the effectiveness of MWCNTs was maximum at ABS-5. For the

low wt% of MWCNTs the distribution of the MWCNTs in the polymer matrix is less efficient that result in higher value of “C”⁴⁷. Now the degrees of entanglements between the polymer matrix and MWCNTs have also been calculated.

Degree of entanglement density

Degree of the entanglement of the polymer composites can also be measured by dynamic mechanical analysis. To determine the degree of entanglement, the value of storage modulus is used as⁴⁸

$$N = \frac{E'}{6RT} \quad (5)$$

Where E' is the storage modulus, R is the universal gas constant, and T is the absolute temperature. The degree of the entanglement increased with increase of wt % of MWCNTs in the ABS matrix. The value of entanglement between ABS and MWCNTs/ABS are shown Figure 5. The entanglement density increased upto ABS-5 and then decreased at the higher loading. In the higher weight % MWCNTs -MWCNTs interaction take place and decreasing the value of the entanglement.

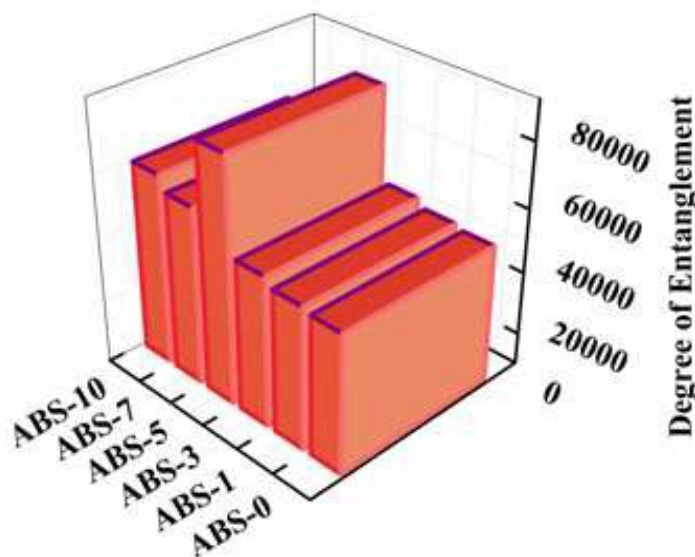


Fig 5. Variation in degree of the entanglement factor with wt. % of MWCNTs in the ABS matrix at 150°C

Table 1. DMA Data (C-Factor and degree of entanglement) for pure ABS and different MWCNTs/ABS Composites

<i>S.No</i>	<i>MWCNTs/ABS composites</i>	<i>Storage modulus(Glassy region)(130 °C) Pa</i>	<i>Storage modulus(rubbery region)(150 °C) Pa</i>	<i>C-Factor</i>	<i>Degree of entanglement (at 150 °C) mol/m³</i>
1)	ABS-0	4.26E9	9.1E8	-	4.31E4
2)	ABS-1	4.75E9	9.34E8	1.086	4.427E4
3)	ABS-3	5.33E9	9.86E8	1.15	4.67E4
4)	ABS-5	5.928E9	1.61E9	0.78	7.6E4
5)	ABS-7	6.68E9	1.17E9	1.22	5.54E4
6)	ABS-10	7.11E9	1.26E9	1.20	5.97E4

Reinforcement efficiency factor

The simplest equation used for calculation of the reinforcement efficiency factor of the composites introduced by Einstein⁴⁹

$$E_c = E_m (1+rV_F) \quad (6)$$

Where E_c , E_m are the storage modulus of the composite and matrix respectively. V_F is the volume fraction of the filler and r is the reinforcement efficiency factor. Figure 6 shows that the reinforcement factor decreased with increase of the volume fraction of the filler upto 5 wt. % of MWCNTs in ABS. The reinforcement factor depends upon the volume fraction of the MWCNTs added in the polymer composites. Figure 6(a) shows that the ABS1 (1 wt. %) have large value of reinforcement. The value of reinforcement is better in ABS5 because the proper dispersion of MWCNTs in ABS polymer and perfect bonding between them. Beyond this loading some of the

agglomeration of the CNTs is found as shown in SEM image (Figure 2b). In figure 6(b) E_c/E_m value at 178°C temperature versus reinforcement factor also clearly shows the bonding concept between the ABS and MWCNTs. The value of E_c/E_m is lowest for ABS 5 sample which shows better dispersion and bonding of CNTs in ABS matrix clearly evident from SEM image (Figure 2a).

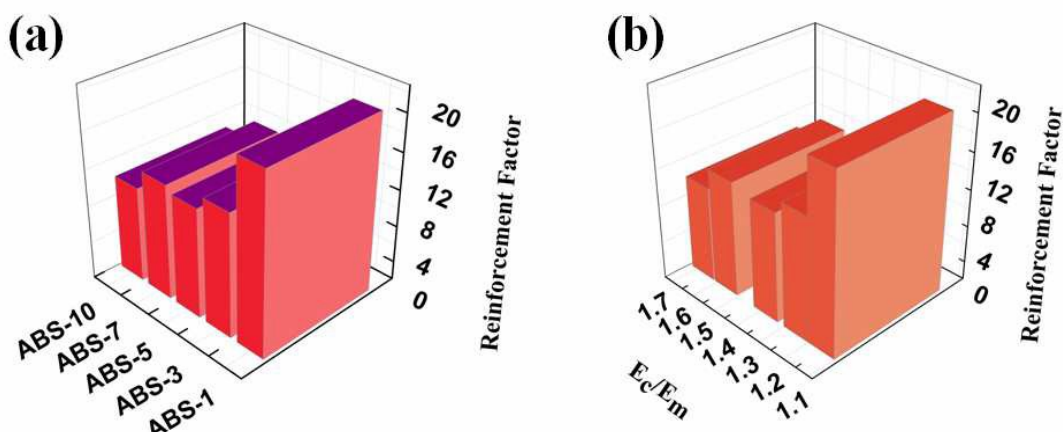


Fig. 6 (a) Variation of Reinforcement factor with wt. % of MWCNTs in the ABS matrix (b) ratio of storage modulus of polymer composites and pure polymer with reinforcement factor

Loss modulus

Loss modulus (E'') measures the maximum heat dissipated per cycle under the deformation. Figure 7 shows that the variation of the loss modulus for different wt% of MWCNTs/ABS nanocomposites with the temperature. It is clear that the addition of MWCNTs in the polymer matrix caused the broadening of the loss modulus peak. This may be attributed to the inhibition of the relaxation process within the composites as a consequence of a higher number of chain segments with addition of MWCNTs⁴⁷.

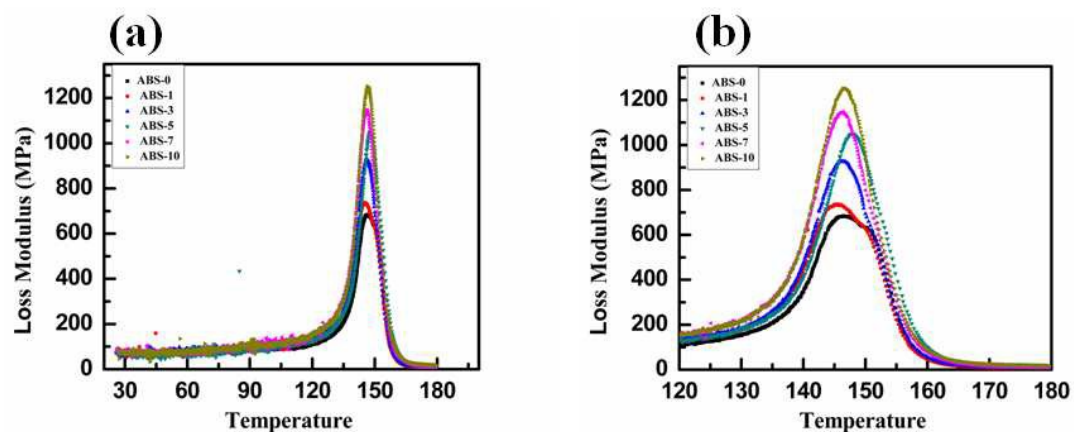


Fig. 7 Variation of (a) loss modulus with temperature (b) zoomed plot between 120 to 180°C for different wt % of MWCNTs/ABS composites

The value of the loss modulus increased with the increase of wt% of MWCNTs in ABS polymer. The higher value of the loss modulus is due to the increase the value of the internal fraction that enhances the dissipation energy. Loss modulus curve reaches the maximum for max. dissipation of a mechanical energy. After that peak, height decreases for the higher temperature as a result of the free movement of the polymer chain. Higher wt% of MWCNTs reduce the flexibility of the composite materials by introducing constraints on the segmental mobility of the polymeric molecules at the relaxation temperatures^{47, 50, 51}. There was an apparent shift in the glass transition T_g toward the higher temperature as increasing the wt% of MWCNTs (ABS-0 to ABS-5). This is attributed primarily due to the segmental immobilization of the matrix chain on the MWCNTs surface³¹. A high value of the loss modulus indicates that the system containing the more restriction at a high degree of the reinforcement⁵².

Damping parameters ($\tan \delta$)

Damping properties of the material provides the balance between the viscous and elastic phase of the polymer composites⁵³. Figure 8 showed that the value of $\tan \delta$ for different wt. % of MWCNTs/ABS nanocomposites were lower than the ABS-0 polymer matrix. As the wt% of MWCNTs increased in the polymer matrix, the value of $\tan \delta$ value decreased.

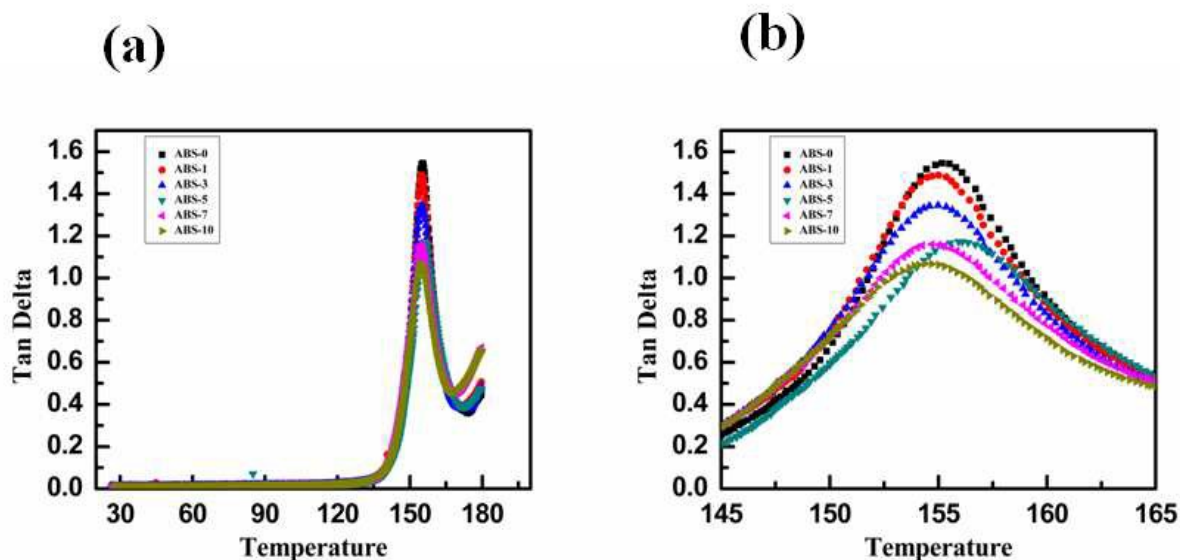


Fig. 8 Variation of (a) Tan delta with temperature plot (b) zoomed part between 145 - 165°C for different wt % of MWCNTs/ABS composites

As the temperature increases, the value of damping goes through the maximum in the transition region and then decreases in the rubbery region. Damping factor is low below the T_g because the thermal energy is insufficient to cause the transition and the rotational motion of the segments and the chain segments are in the frozen state⁵⁴. And the deformation is the primary mechanism of the elastic and the molecular slips resulting in the viscous flow⁴⁷. In the rubbery region, the molecular segments are quite free to move. These motions are also the concern with cooperative diffusion motion of the molecular chain segments.

Adhesion factor

An adhesion factor (A) is determined from the damping factor of the polymer matrix and polymer composites as the function as the volume fraction of the filler and temperature⁵⁵. Damping factor of polymer composite can be expressed in the term volume fraction and the damping factor within the composites system.⁵⁶

$$\tan\delta_c = \phi_f \tan\delta_f + \phi_i \tan\delta_i + \phi_p \tan\delta_p \quad (7)$$

Subscript c, f, i, and p stand for the composites, filler, interface of polymer and polymer matrix respectively. By assuming the filler damping may be considered a low value and the interface

volume fraction should be lower and neglected if compared to its filler and matrix counterpart, equation (7) become.

$$\phi_f \tan \delta_f = 0$$

Then equation (7) become

$$\tan \delta_c = \phi_i \tan \delta_i + \phi_p \tan \delta_p \quad (8)$$

Also we know $\phi_f + \phi_p = 1$, substituting the equation (8) and rearrange the equation

$$\frac{\tan \delta_c}{\tan \delta_p} = (1 - \phi_i) \times (1 + A) \quad (9)$$

The adhesion factor 'A' can be expressed in terms of the relative damping of the composite and the polymer and the volume fraction of the filler at a given temperature. This assumption would be reasonable only if the development of a transcrystallinity layer at the composite interphase could be neglected.

$$A = \frac{1}{(1 - \phi_f)} \frac{\tan \delta_c}{\tan \delta_p} - 1 \quad (10)$$

Correa et al.⁵⁷ have studied the adhesion factor of the polymer composites. Higher the degree of the interaction between MWCNTs and matrix, i.e lower the value of adhesion factors.

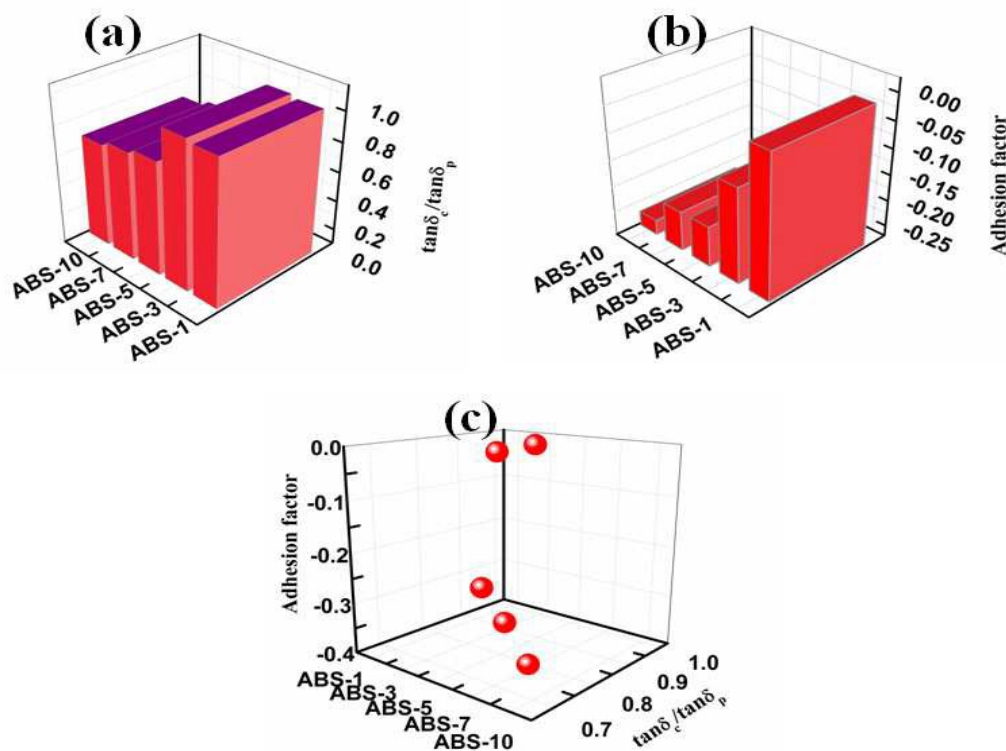


Fig. 9 Variation of (a) Ratio of the damping factor of the composite and polymer (b) adhesion factor versus wt.% of MWCNTs and (c) 3D diagram of adhesion factor and Ratio of the damping factor of the composite and polymer for different wt % of MWCNTs/ABS composites

MWCNTs –ABS matrix interphase adhesion

DMA characterized the filler matrix interphase in the polymer composites by assuming that the composites dissipation not only attribute to the matrix phase but also depends upon the filler matrix interaction. The interaction between filler and polymer matrix interface tends to form the immobilized interface. The nanofiller themselves do not contribute to the damping but they depend upon the polymer matrix. The composite's dissipation factor can be calculated from the following relation.⁵⁸

$$\frac{\tan\delta_c}{\tan\delta_p} = 1-bV_F \quad (11)$$

Where $\tan\delta_c$, and $\tan\delta_p$ is the damping factor of the composites and polymer matrix respectively. V_F is the volume fraction of the filler. “b” is a parameter introduced the correct volume fraction of the reinforcement because the formation of the layer of immobilized interphase resulting from filler- matrix interaction. The value of “b” reaches the max. value at 5% wt of MWCNTs as shown in figure 10. After that, it starts decreasing due to MWCNTs – MWCNTs interaction.

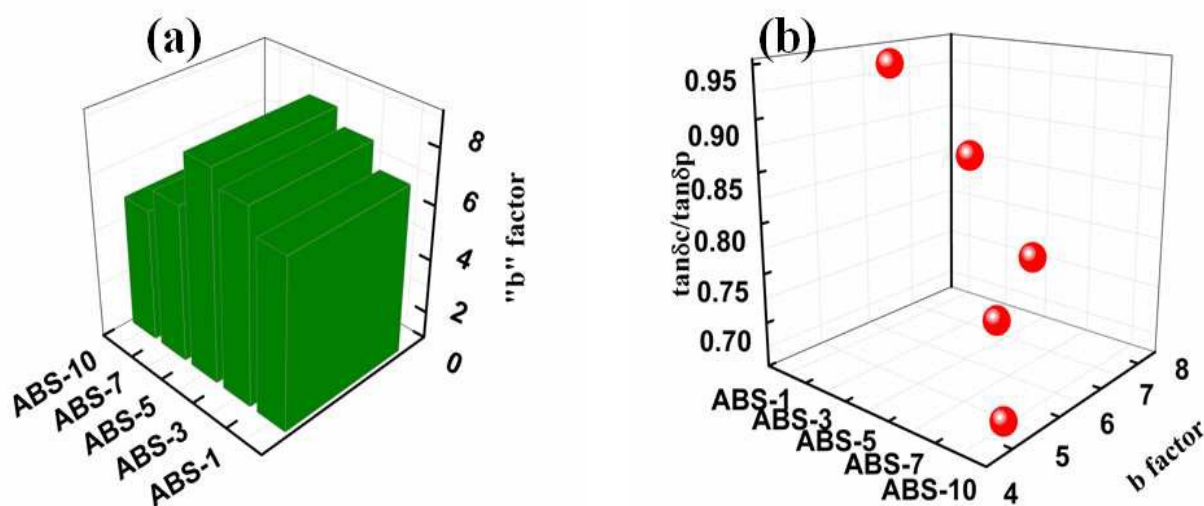


Fig. 10. Variation of (a) matrix interphase factor b and (b) 3D diagram for damping behaviour and b-factor for different wt % of MWCNTs/ABS composites

MWCNTs/ABS stiffness calculation

Figure 11 shows the variation in the ratio of the sample total stiffness regarding the amount of the MWCNTs loading. The stiffness of the composites enhanced rapidly with MWCNTs loading. Stiffness of the polymer composites depends upon the amount of MWCNTs and length of carbon nanotubes⁵⁹⁻⁶¹

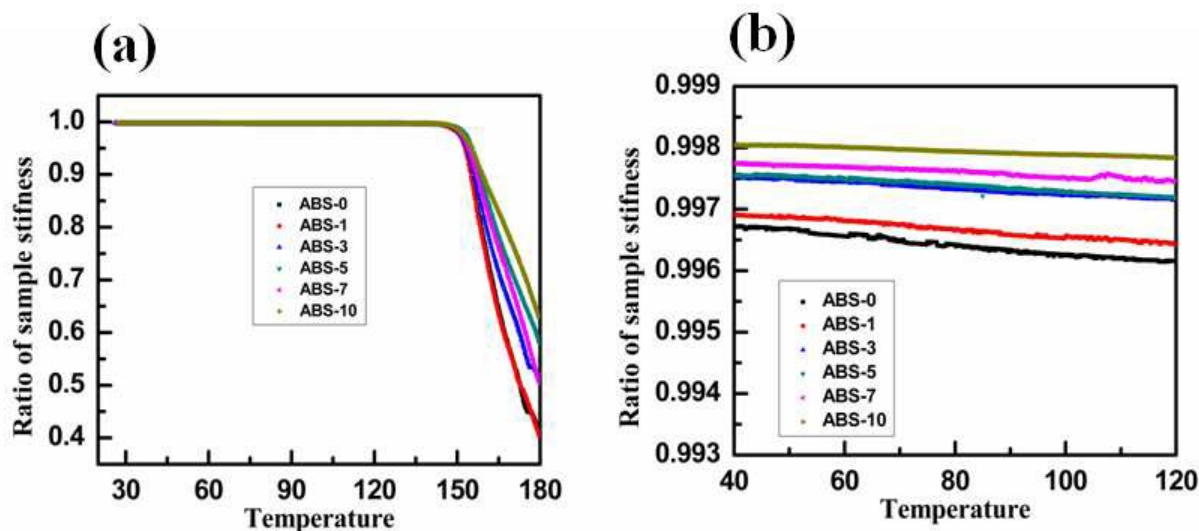


Fig.11 (a) Ratio of the sample stiffness vs. temperature plot for different wt % of MWCNTs/ABS composites (b) at the lower range of the temperature scale (zoom

Cole- Cole analysis

Structural properties changes from the addition of MWCNTs in cross linked polymers matrix can be studied using Cole-Cole method. The dissipation or loss factor measured during dynamic mechanical measurements is directly analogous to the $\tan\delta$ function relevant to the dynamic mechanical testing. Cole Cole is a particular treatment of dielectric relaxation data, obtained by plotting the E'' against E' , each point corresponding to one frequency.

The dynamic mechanical properties examined as a function of temperature and frequencies are represented on the Cole-Cole complex plane. Figure 12 shows the Cole-Cole plots of various composite systems, where the loss modulus are plotted as a function of the storage modulus at a frequency of 1 Hz.

The nature of Cole-Cole plot is reported to be indicative of the nature of the system. The homogeneous polymeric systems are reported to show a semicircle diagram whilst the two-phase systems show not perfect semicircle (elliptical path)^{62, 63}. On analysing the Cole-Cole plots of the present composite systems it is seen that the curves show the shape of imperfect semicircles. The shape of the curves thus points towards the good adhesion.

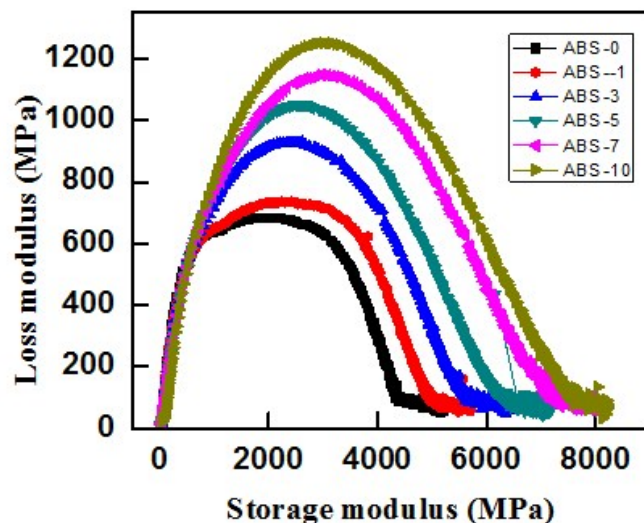


Fig. 12 Cole-Cole plots of pure ABS and MWCNTs/ABS composites

DMA of pure ABS and MWCNTs/ABS composites studied the degree of entanglement, coefficient of “C” factor and adhesion factor. All these properties showed that 5 wt. % of MWCNTs loading are sufficient for the better enhancement of the properties of ABS matrix. After 5 wt. % MWCNTs-MWCNTs interactions were taken place.

Conclusion

Dynamic mechanical analysis of pure ABS and ABS-MWCNTs composites were studied. The results showed that addition of MWCNTs into ABS matrix increases the value of storage, loss modulus and decreases the value of damping factor. The improvement of the storage modulus by the addition of MWCNTs provided the better load bearing capacity for the composite. The glass transition temperature of the composites shifted to the higher region as increases the wt. % of MWCNTs. The coefficient of “C” factor, adhesion factor, reinforcement factor, b factor and degree of entanglement has been studied with the incorporation of MWCNT in ABS matrix by dynamic mechanical analysis. It has been found that degree of entanglement increases upto 5 wt.% MWCNT loading and beyond this loading it decreased. Similar, b factor was also increased upto 5 wt. loading in the ABS and beyond this loading it was decreased. C factor was decreased with the increase of MWCNT loading upto 5 wt.% loading and then starts increasing beyond this

loading. Reinforcement factor was decreased upto 5 wt. % loading and then start increasing beyond this loading. The results from all these factors show that 5 wt% loading of MWCNTs in ABS matrix is sufficient for the better improvement in the properties of MWCNT/ABS composites. DMA can provide a significant insight to design the mechanically strong material with the incorporation of MWCNTs.

Acknowledgement:

The authors wish to express their gratitude to DNPL to accord this permission to publish the result. Authors are also thankful to Mr. K.N. Sood and Mr. Jay Tawale for SEM measurement and Mr. Dinesh Singh for TEM measurement. The studies were carried out under the CSIR-Network project (D-NEED, PSC0109).

References

1. S. Pande, B. P. Singh and R. B. Mathur, in *Polymer Nanotube Nanocomposites: Synthesis, Properties, and Applications, Second Edition*, John Wiley & Sons, Inc., 2014, pp. 333-364.
2. R.B. Mathur, S. Pande and B.P Singh, *Polymer Nanotube Nanocomposites: Synthesis, Properties, and Applications*, 2010, 11, 177.
3. D. Romanzini, A. Lavoratti, H. L. Ornaghi, S. C. Amico and A. J. Zattera, *Materials & Design*, 2013, 47, 9-15.
4. S. N. Cassu and M. I. Felisberti, *Química nova*, 2005, 28, 255-263.
5. H. L. Ornaghi, V. Pistor and A. J. Zattera, *Journal of Non-Crystalline Solids*, 2012, 358, 427-432.
6. V. Pistor, F. G. Ornaghi, H. L. Ornaghi and A. J. Zattera, *Materials Science and Engineering: A*, 2012, 532, 339-345.
7. O. M. Istrate, K. R. Paton, U. Khan, A. O'Neill, A. P. Bell and J. N. Coleman, *Carbon*, 2014, 78, 243-249.
8. A. Babal, R. Gupta, B. P. Singh, V. N. Singh, R. B. Mathur and S. R. Dhakate, *RSC Advances*, 2014, 4, 64649-64658.
9. A. Babal, R. Gupta, B. P. Singh and S. R. Dhakate, *RSC Advances*, 2015, 5, 43462-43472.
10. T. K. Gupta, B. P. Singh, R. K. Tripathi, S. R. Dhakate, V. N. Singh, O. Panwar and R. B. Mathur, *RSC Advances*, 2015, 5, 16921-16930.
11. T. K. Gupta, B. P. Singh, V. N. Singh, S. Teotia, A. P. Singh, I. Elizabeth, S. R. Dhakate, S. Dhawan and R. Mathur, *Journal of Materials Chemistry A*, 2014, 2, 4256-4263.
12. D. Hanlon, C. Backes, E. Doherty, C. S. Cucinotta, N. C. Berner, C. Boland, K. Lee, P. Lynch, Z. Gholamvand and A. Harvey, *arXiv preprint arXiv:1501.01881*, 2015.
13. J.-M. Thomassin, M. Trifkovic, W. Alkarmo, C. Detrembleur, C. Jérôme and C. Macosko, *Macromolecules*, 2014, 47, 2149-2155.
14. T. K. Gupta, B. P. Singh, S. R. Dhakate, V. N. Singh and R. B. Mathur, *Journal of Materials Chemistry A*, 2013, 1, 9138-9149.
15. R. Haggenmueller, H. Gommans, A. Rinzler, J. E. Fischer and K. Winey, *Chemical physics letters*, 2000, 330, 219-225.

16. D. Spasevska, G. Leal, M. Fernández, J. B. Gilev, M. Paulis and R. Tomovska, *RSC Advances*, 2015, 5, 16414-16421.
17. H. Peng, G. Ma, K. Sun, J. Mu, H. Wang and Z. Lei, *Journal of Materials Chemistry A*, 2014, 2, 3303-3307.
18. C. Liao, Q. Wu, T. Su, D. Zhang, Q. Wu and Q. Wang, *ACS applied materials & interfaces*, 2014, 6, 1356-1360.
19. S. P. Pawar, D. A. Marathe, K. Pattabhi and S. Bose, *Journal of Materials Chemistry A*, 2015, 3, 656-669.
20. B.P Singh, D. Saket, A. Singh, S. Pati, T. Gupta, V. Singh, S. Dhakate, S. Dhawan, R. Kotnala and R. Mathur, *J. Mater. Chem. A*, 2015, 3, 13203-13209.
21. H. J. Salavagione, A. M. Díez-Pascual, E. Lázaro, S. Vera and M. A. Gómez-Fatou, *Journal of Materials Chemistry A*, 2014, 2, 14289-14328.
22. M. Janani, P. Srikrishnarka, S. V. Nair and A. S. Nair, *Journal of Materials Chemistry A*, 2015, 3, 17914-17938.
23. Y. Yao, H. Xiao, P. Wang, P. Su, Z. Shao and Q. Yang, *Journal of Materials Chemistry A*, 2014, 2, 11768-11775.
24. S. Teotia, B. P. Singh, I. Elizabeth, V. N. Singh, R. Ravikumar, A. P. Singh, S. Gopukumar, S. Dhawan, A. Srivastava and R.B. Mathur, *RSC Advances*, 2014, 4, 33168-33174.
25. S. Pande, A. Chaudhary, D. Patel, B. P. Singh and R. B. Mathur, *RSC Advances*, 2014, 4, 13839-13849.
26. J. Jyoti, S. Basu, B.P Singh and S. Dhakate, *Composites Part B: Engineering*, 2015.
27. C. Wei, *Applied physics letters*, 2006, 88, 093108.
28. V. Chaudary, Bhanu Pratap Singh, Satish Teotia, Ttejendra K. Gupta, Vidya N. Singh, Sankay R. Dhakate, Rakesh B.Mathur, *Advanced Material Letter*, 2015, 6, 104-113.
29. B.P Singh, V. Choudhary, P. Saini, S. Pande, V. Singh and R. Mathur, *Journal of Nanoparticle Research*, 2013, 15, 1-12.
30. B.P Singh, K. Saini, V. Choudhary, S. Teotia, S. Pande, P. Saini and R. Mathur, *Journal of Nanoparticle Research*, 2014, 16, 1-11.
31. P. Joseph, G. Mathew, K. Joseph, G. Groeninckx and S. Thomas, *Composites Part A: applied science and manufacturing*, 2003, 34, 275-290.
32. W. Goertzen and M. Kessler, *Composites Part B: Engineering*, 2007, 38, 1-9.
33. T. Hatakeyama and F. Quinn, *Thermal Analysis*, 1994.
34. J. Otaigbe, *Polymer Engineering & Science*, 1991, 31, 104-109.
35. B. Harris, O. Braddell, D. Almond, C. Lefebvre and J. Verbist, *Journal of Materials Science*, 1993, 28, 3353-3366.
36. K. E. Verghese, R. Jensen, J. Lesko and T. Ward, *Polymer*, 2001, 42, 1633-1645.
37. A. Etaati, S. Pather, Z. Fang and H. Wang, *Composites Part B: Engineering*, 2014, 62, 19-28.
38. M. Jawaid, H. A. Khalil, A. Hassan, R. Dunganani and A. Hadiyane, *Composites Part B: Engineering*, 2013, 45, 619-624.
39. Y. Karaduman, M. Sayeed, L. Onal and A. Rawal, *Composites Part B: Engineering*, 2014, 67, 111-118.
40. K. S. Khare and R. Khare, *The Journal of Physical Chemistry B*, 2013, 117, 7444-7454.
41. P. Jyotishkumar, E. Abraham, S. M. George, E. Elias, J. Pionteck, P. Moldenaers and S. Thomas, *Journal of applied polymer science*, 2013, 127, 3093-3103.
42. G. Hatui, G. C. Nayak, C. K. Das and S. B. Yadaw, *Journal of applied polymer science*, 2013, 129, 57-64.
43. R.B. Mathur, S. Chatterjee and B.P Singh, *Composites Science and Technology*, 2008, 68, 1608-1615.

44. J. M. Faulstich de Paiva and E. Frollini, *Macromolecular Materials and Engineering*, 2006, 291, 405-417.
45. C. Komalan, K. George, P. Kumar, K. Varughese and S. Thomas, *Express Polym Lett*, 2007, 1, 641-653.
46. L. A. Pothan, Z. Oommen and S. Thomas, *Composites Science and Technology*, 2003, 63, 283-293.
47. N. Hameed, P. Sreekumar, B. Francis, W. Yang and S. Thomas, *Composites Part A: applied science and manufacturing*, 2007, 38, 2422-2432.
48. Z. Oommen, G. Groeninckx and S. Thomas, *Journal of Polymer Science Part B: Polymer Physics*, 2000, 38, 525-536.
49. A. Einstein, Dover, New-York, 1956.
50. M. A. López-Manchado, J. Biagitti and J. M. Kenny, *Polymer Composites*, 2002, 23, 779-789.
51. S. Mohanty, S. K. Verma and S. K. Nayak, *Composites Science and Technology*, 2006, 66, 538-547.
52. J. H. S. A. Júnior, H. L. O. Júnior, S. C. Amico and F. D. R. Amado, *Materials & Design*, 2012, 42, 111-117.
53. H. Gu, *Materials & Design*, 2009, 30, 2774-2777.
54. J. D. Ferry, *Viscoelastic properties of polymers*, John Wiley & Sons, 1980.
55. L. A. Pothan, S. Thomas and G. Groeninckx, *Composites Part A: applied science and manufacturing*, 2006, 37, 1260-1269.
56. J. Kubat, M. Rigdahl and M. Welander, *Journal of applied polymer science*, 1990, 39, 1527-1539.
57. C. Correa, C. Razzino and E. Hage, *Journal of Thermoplastic Composite Materials*, 2007, 20, 323-339.
58. J. Sarasua and J. Pouyet, *Journal of Thermoplastic Composite Materials*, 1998, 11, 2-21.
59. K. W. Putz, M. J. Palmeri, R. B. Cohn, R. Andrews and L. C. Brinson, *Macromolecules*, 2008, 41, 6752-6756.
60. L. Schadler, S. Giannaris and P. Ajayan, *Applied physics letters*, 1998, 73, 3842-3844.
61. J. N. Coleman, U. Khan, W. J. Blau and Y. K. Gun'ko, *Carbon*, 2006, 44, 1624-1652.
62. R. F. Landel and L. E. Nielsen, *Mechanical properties of polymers and composites*, CRC Press, 1993.
63. R. Chandra, S. Singh and K. Gupta, *Composite Structures*, 1999, 46, 41-51.

Graphical Abstract

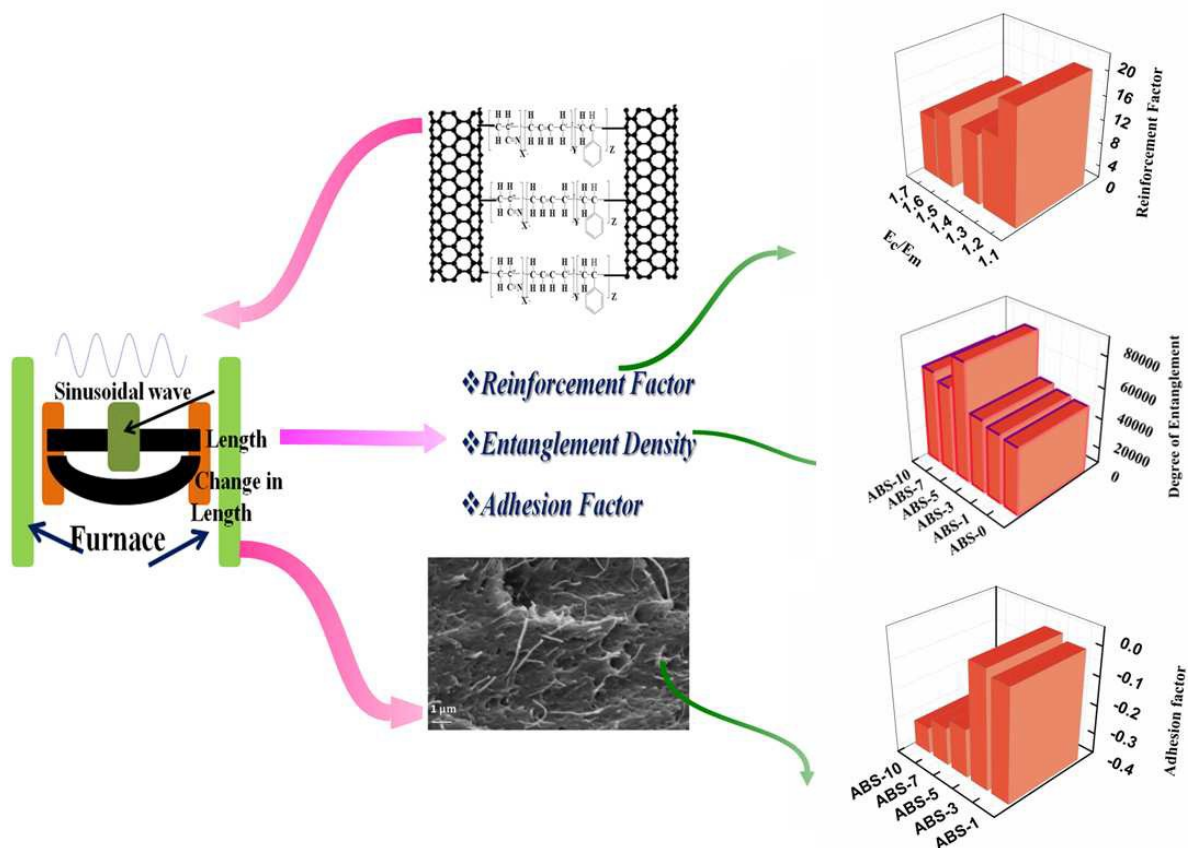
Dynamic Mechanical Properties of Multiwall Carbon Nanotube Reinforced ABS Composites and its Correlation with Entanglement Density, Adhesion, Reinforcement and C Factor

Jeevan Jyoti^{1,2}, Bhanu Pratap Singh^{1,2*}, Abhishek K. Arya¹, S.R Dhakate¹

¹Physics and Engineering of Carbon, Division of Materials Physics and Engineering

²Academy of Scientific and Innovative Research (AcSIR),

CSIR-National Physical Laboratory, New Delhi-11012, India



Herein, Dynamic Mechanical Properties of Multiwall Carbon Nanotube Reinforced ABS Composites have been studied with dynamic mechanical analyzer and the results have been correlated with Entanglement Density, Adhesion, Reinforcement and C Factor.